Numerical Study of SF6 arc with Copper Contamination

Vui-Kien Liau*, Byeong-Yoon Lee[†], Ki-Dong Song* and Kyong-Yop Park*

Abstract - The present model of a SF6 arc accounts for the copper vapour contamination from the electrodes inside a Laval nozzle of a circuit breaker. Steady state simulations have been done for the arc with electrode gap of 60mm and DC electric current of 500A, 1000A and 1500A for both cases with and without copper contamination. The effects of electrode polarity are considered for the arc current of 1000A. It was found out that evaporation of copper from the anode results in a cooling of the arc in a region close to the electrodes. The electrical potential across the electrodes is not sensitive to the presence of copper vapour, typically less than 4% difference. Transient analysis has been done in order to obtain the arc properties at current zero. The arc current is increased linearly from -1000 to 0A when the upstream electrode is cathode with constant dI/dt of 27.0A/μs (or decreased linearly from 1000 to 0A when upstream electrode is anode). It has been predicted that the presence of copper vapour reduces the interruption capability of the breaker.

Keywords: arc simulation, circuit breaker, SF6

1. Introduction

During the operation of an SF6 circuit breaker, the electrodes may be eroded due to the presence of high temperature arc [1]. The erosion process depends on how long the arc is present, the magnitude of the arc current as well as the composition of the electrodes. The main erosion process is the evaporation of the contacts, and is considered in the present investigation. The ejection of liquid droplets from the electrodes is not considered. When both the current is high and arcing duration is long, the temperature of electrodes surface increases to the melting temperature and then partially vaporised. As the results, the arc burns in the mixture of metallic vapour and SF6. The presence of the metallic vapour not only changes the transport properties and radiation loss of the arc, it also adds the mass, momentum and energy to the overall system. Bouaziz et. al [2] showed that the radiation loss increases significantly and the electrical conductivity is strongly dependent on the metallic vapour concentration especially at low temperature below 10,000K. The presence of metallic vapour enables the arc to be cooled through enhanced radiation during the intense current phase, and prevents the effective cut-off occurring when the voltage is re-established at current zero, hence changes the interruption capability of the circuit breaker.

However, until now, there are very few quantitative

experimental and theoretical studies of the influence of metallic vapours on the performance of SF6 circuit breaker in the literature. Computer modeling without the consideration of copper vapour has been performed by [3], [4, 5, 6]. One of the difficulties in experimental investigation arises from the fact that the arc burning in the mixture of SF6 and metallic vapours is unstable, hence difficult to obtain reproducible measurements with precision. Zhang et. al [7] performed the numerical simulation of SF6 arc with copper vapour in a supersonic nozzle under steady state conditions. Bouaziz et. al [2] performed experimental and theoretical study of the influence of copper vapour on a SF6 arc in an inductively coupled torch. Ciabanu et. al [8] has undertaken an experimental and theoretical study of copper electrode vaporization in a medium-voltage circuit breaker, which showed that there is a strong emissive copper zone at the region around the electrodes. Ikeda et. al [9] measured the temperature of the SF6 arc with W-Cu electrodes and found out that the arc temperature is about 16000K in the metallic vapour rich region, and 18000K in the surrounding plasma.

In most applications in practice, the electrodes are made of copper or copper/tungsten alloy. By employing different material for electrodes, the material properties (such as melting point, thermal conductivity) differ and this can affect the electrode evaporation rate, and hence the circuit breaker performance [10]. For simplicity, in the current investigation, copper electrode is chosen. Computer simulation of the arc has been done using a commercial computational fluid dynamics (CFD) software "PHOENICS" version 3.4. The simulations were carried out in two steps, first steady state arc simulation, followed by transient arc

simulation before current zero.

The paper is organized in the following order. Section 2 describes the formulation and governing equations of the arc model. In section 3, the computational results for arc under steady state current of 500A, 1000A and 1500A and the transient arc simulation of the arc at current zero are presented and discussed. The effects of the polarities of the electrodes are also presented. Finally, conclusions are drawn in Section 4.

2. Mathematical Model

2.1 Governing equations in the plasma domain

The arc plasma is assumed to be axisymmetric, turbulent and under local thermodynamic equilibrium (LTE). Due to the high pressure, it is assumed that the copper vapour and SF6 gas are completely mixed and attain the same velocity. The following set of equations was used for the modelling of the arc:

Continuity equation

$$\frac{\partial \rho}{\partial t} + \nabla \cdot (\rho \vec{V}) = 0 \tag{1}$$

Momentum conservation equations

$$\frac{\partial}{\partial t}(\rho v) + \nabla \cdot (\rho \vec{V} v) - \nabla \cdot ((\mu_l + \mu_t)\nabla v) = -\frac{\partial P}{\partial r} + J_z B_\theta +$$

viscous terms $\tag{2}$

$$\frac{\partial}{\partial t}(\rho w) + \nabla \cdot (\rho \vec{V} w) - \nabla \cdot ((\mu_l + \mu_t)\nabla w) = -\frac{\partial P}{\partial z} + J_r B_\theta +$$

viscous terms $\tag{3}$

Energy conservation equation

$$\frac{\partial}{\partial t}(\rho h) + \nabla \cdot (\rho \vec{V} h) - \nabla \cdot \left(\left(\frac{k_l + k_t}{c_p} \right) \nabla h \right) = \sigma E^2 - q +$$

viscous dissipation $\tag{4}$

Metal vapour mass continuity

$$\frac{\partial}{\partial t}(\rho c_i) + \nabla \cdot (\rho \vec{V} c_i) - \nabla \cdot (\rho (D_l + D_t)\nabla c_i) = 0 \tag{5}$$

where P is the local pressure, ρ the mass density, $\vec{V}$ the velocity vector of the plasma, v and w the radial and axial component of the velocity, μ the viscosity, J_r and J_z the radial and axial current density, B_θ the azimuthal component of the magnetic field, h the enthalpy, k the thermal conductivity, σ the electrical conductivity, c_p the

specific heat at constant pressure, E the electric field, q the radiation loss, c_m the mass fraction of copper vapour in the plasma and D the diffusion coefficient of the copper vapour. The subscript l and t represent the laminar and turbulent components respectively.

The mass fraction is defined as

$$c_i = \frac{n_{Cu} M_{Cu}}{n_{Cu} M_{Cu} + n_{SF_6} M_{SF_6}} \tag{6}$$

where n and M are respectively the molar number and molar mass.

The diffusion coefficient in the copper vapour mass continuity equation can be written as [7]:

$$D_l = \frac{\mu_l}{\rho} \qquad D_t = \frac{\mu_t}{\rho} \tag{7}$$

Current continuity

$$\nabla \cdot (\sigma \nabla \varphi) = 0 \tag{8}$$

where φ is the electrical potential.

Ampere's Law

$$\frac{1}{r} \frac{\partial}{\partial r}(r B_\theta) = \mu_0 J_z \tag{9}$$

where μ_0 is the permeability of free space ($4\pi \times 10^{-7}$H/m).

2.2 Governing equations in the electrode domain

Within the electrode region, only the energy equation is solved. The ohmic heating is ignored as the electrical conductivity of the copper electrode is very high.

$$\frac{\partial}{\partial t}(\rho c_{p,m} T_m) - \nabla \cdot (k_m \nabla T_m) = 0 \tag{10}$$

where the subscript m represents the properties of the electrode material.

2.3 Arc-electrode Interface

The interaction between the arc and the electrodes is very complex. From the surface of electrode, there is a sheath region, followed by quasi-neutral non-equilibrium region. The energy balance across the electrodes is very important in calculating the copper evaporation rate. For the current investigation, the method proposed by [7] is used in determining the copper vapour evaporation process from the energy balance at the electrodes surface. The

physical processes considered are summarised as follow:

Arc-cathode

The cathode spot is considered to be a circular area with maximum radius of 1.5mm. The current density in the cathode spot is represented by the following exponential function according to Hsu et. Al [11]:

$$J = J_{max} \exp(-br), r \leq 1.5mm$$
$$J = 0 \qquad , r > 1.5mm \qquad (11)$$

where J_{max} = $2.0 \times 10^8 Am^{-2}$. The coefficient b is set according to the arc current. For arc current magnitude I between 0.1A to 1500A, b can be computed according to the following fitted formulae:

$$b = A_0 + A_1 \ln(I) + A_2 \ln(I)^2 + A_3 \ln(I)^3$$
$$+ A_4 \ln(I)^4 + A_5 \ln(I)^5 \qquad (12)$$

where A_0=3.5002×10⁴, A_1=-1.6768×10⁴, A_2=3.6663×10³, A_3=-4.3582×10², A_4=2.6296×10¹, A_5=6.3166×10⁻¹

Outside the cathode spot, only thermal conduction transfers the energy from the arc to the electrode. In front of the cathode spot, the energy flux brought to the surface by thermal conduction from the arc $q_{cond,arc}$ and ion bombardment heating q_{ion} is balanced out by electron emission cooling q_{not} (Nottingham effect), cathode material vaporization q_{vap} and thermal conduction through the electrode bulk $q_{cond,m}$.

$$q_{cond,arc} + q_{ion} = q_{not} + q_{vap} + q_{cond,m} \qquad (13)$$

where

$$q_{ion} = J_i \left(V_c + V_i - \Phi_c + \frac{5kT_c}{2e} \right) \qquad (13a)$$

$$q_{not} = |J_e| \Phi_c \qquad (13b)$$

$$q_{cond,arc} = -\left(\frac{k_l + k_t}{c_p} \right) \frac{\partial h}{\partial z} \qquad (13c)$$

$$q_{cond,m} = -k_m \frac{\partial T}{\partial z} \qquad (13d)$$

$$q_{vap} = h_v \dot{m} \qquad (13e)$$

V_c is the voltage drop in the cathode sheath (assumed to be 17.5V) , V_i the ionization energy of the plasma gas (7.73V), J_i and J_e the ion and electron current density, Φ_c the work function of the cathode material (4.5V), k the Boltzmann constant, e the magnitude of electronic charge, T_c the cathode spot temperature, h_v the sum of latent heat of

fusion and vaporisation (5204kJ/kg) and $\dot{m}$ the rate of vaporisation of electrode.

Since the model assumes LTE, it is not possible to calculate the J_e and J_i. As an approximation, $|J_i|/|J_e| = 0.78$ and $J = |J_i| + |J_e|$. The momentum flux produced by the vapour jet is $\dot{m}^2 / \rho$ and the enthalpy flux is $\dot{m}h_{vg} + |j_e||V_c|$, h_{vg} is the copper vapour enthalpy at boiling point.

Arc-anode

When the temperature at the anode surface is higher than the melting point (1356K), the energy flux gained from incident electron heating q_e and thermal conduction from the arc $q_{cond,arc}$ is balanced by the anode material vaporization q_{vap} and thermal conduction through the electrode bulk $q_{cond,m}$. If the anode surface temperature is below the melting point, no electrode vaporisation will occur and only conjugate heat transfer is present. Since the non-LTE layer between the arc and the electrode is not considered, the temperature of the arcing gas adjacent to the anode to be high enough to maintain current continuity. Hence the metal vapour from the anode is heated up in the non-LTE region by the energy flux approaching the anode surface before it enters into the arc column. The energy balance can be written as:

$$\dot{m}h_v + \dot{m}(h_g - h_v) = q_{cond,arc} + q_e - q_{cond,m} \qquad (14)$$

where

$$q_e = |J_a| \left(\frac{5k}{2e}(T_g - T_a) + V_a + \Phi_a \right) \qquad (14a)$$

J_a is the current density just in front of the anode surface, T_a the anode temperature, T_g the gas temperature just in front of the anode, V_a the anode fall (assumed to be 2.5V) and Φ_a the work function of the anode material (4.5V).

2.4 Thermodynamic and Transport properties

The thermodynamic properties of the gas mixture are calculated from Coufal [11]. The transport properties are obtained from [12, 13]. The semi-experimental radiation model [14] has been used to calculate the radiation transport in the energy equation, and the net emission coefficient from [15] is used. Turbulence modelling is done according to [16] and the turbulent viscosity is calculated by:

$$\mu_t = \rho l_m^2 \left(2\left(\frac{v}{r}\right)^2 + \left(\frac{\partial w}{\partial r} + \frac{\partial v}{\partial z}\right)^2 \right) \qquad (15)$$

where l_m is the mixing length defined as $l_m = c\delta$, c is the

turbulent parameter and δ the thermal radius of the arc. c is set to 0.10 as determined from [17]

2.5 Computational Domain and boundary conditions

The computational domain is shown in Fig. 1. The overall length of the nozzle is 68.75mm, with inlet diameter of 25mm, outlet diameter of 38.4mm and nozzle throat diameter of 12.50mm. The throat position is located at 15.63mm away from the inlet plane. There are two electrodes with the diameter of 4mm. The electrode gap is 60mm.

At the nozzle inlet, the mass, momentum and enthalpy fluxes are determined assuming isentropic flow of gas with temperature 300K and stagnation pressure of 3.75MPa. At the nozzle outlet, a static pressure of 0.3MPa is set. The electrical potential of the downstream electrode is set to 0V, while the potential of the upstream electrode is iteratively adjusted according to the arc current. At outer boundary of the simulation domain, the gradient of the electrical potential is set to zero. The nozzle wall is assumed to be adiabatic with no ablation. There are all together 140 and 155 cells in the radial and axial direction respectively.
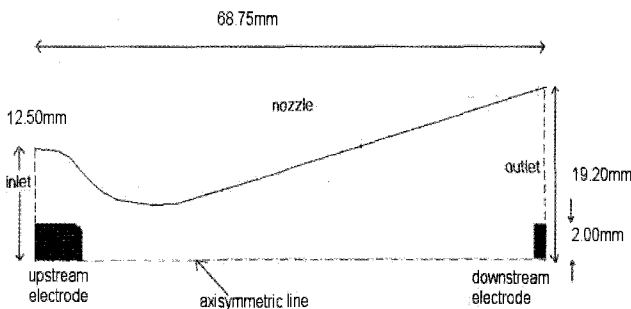
**Fig. 1** Schematic diagram of the computational domain of the system

3. Results and Discussion

Steady state simulations of DC arc current of 500A, 1000A and 1500A has been performed with the effects of electrode evaporation. The effects of electrode polarity and the case without electrode evaporation have been computed for the case of 1000A. Fig. 2 shows the arc temperature distribution with electrical potential lines for the case of 1000A. The upstream electrode is set as cathode in this case. The maximum temperature is around 21000K, and the electrical potential difference between the electrodes is 874V. Inside the arc core, the electric field is axially dominant and radially uniform. Below 10000K, the electric field has substantial radial component. The arc expanded from upstream electrode to downstream electrode.
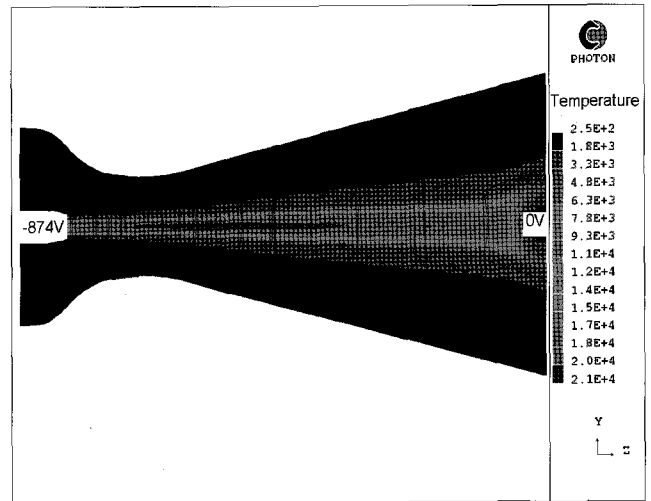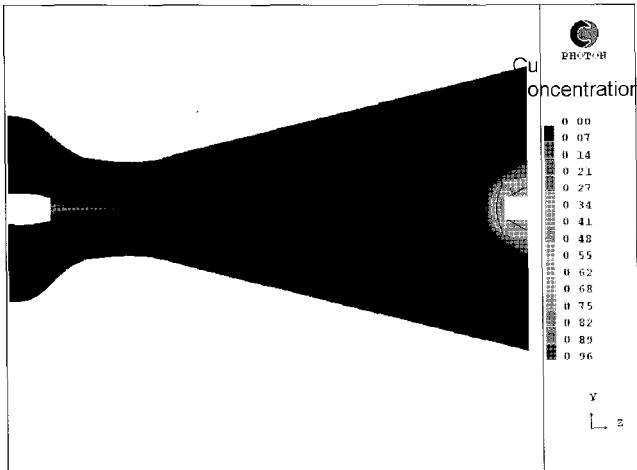

Fig. 2 The temperature distribution of the arc, I=1000A. The electrical potential contour is shown in the same diagram. The upstream electrode is set as cathode

Fig. 3 shows the velocity vector under the same condition. The maximum velocity attained is around 4300m/s. The mass concentration of copper vapour of the arc is shown in Fig. 4. The temperature contours of 2000K and 10000K are shown in the same diagram. In the region very close to the electrodes, the arc burns in almost pure copper vapour. The mass concentration however decreases rapidly away from the upstream electrodes due to the accelerating axial flow and strong turbulent diffusion. The mass concentration at the downstream electrode cannot diffuse against the high speed flow of gas around 4000m/s. The arc attained the highest temperature when the mass concentration of copper vapour is negligible in the region around the nozzle throat.
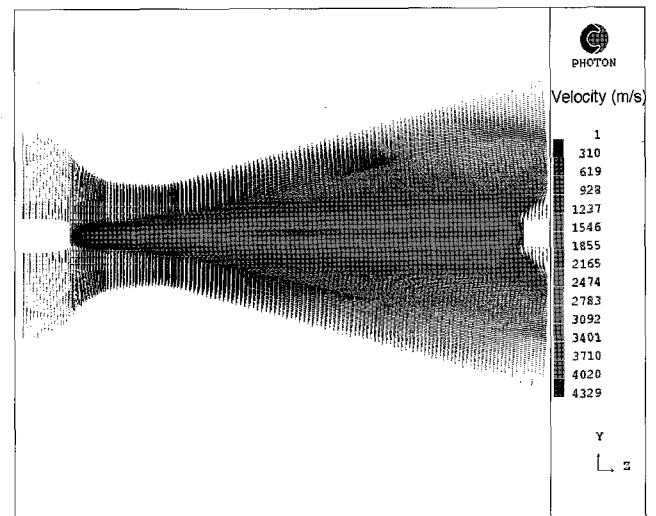

**Fig. 3** The velocity vector of the arc, I=1000A. The upstream electrode is set as cathode

Fig. 4 The distribution of mass concentration of copper vapour, I=1000A. The temperature contours of 2000 and 10000K is shown in the same diagram. The upstream electrode is set as cathode

Fig. 5 shows the arc radius along the axial direction. The arc radius is defined as the radial distance from the axis to the position of 2000K isotherm. The radial power density at nozzle throat with current of 1000A is shown in Fig. 6. Fig. 7 shows the radial distribution of the mass concentration of copper vapour at nozzle throat, while Fig. 8 plots the axial distribution of the mass concentration on the axis. The arc radius increases along the axis, and is proportional to the arc current. The higher the arc current, the higher evaporation rate and the mass concentration of copper vapour increases as shown in Fig.s7 and 8. Typically, when the upstream electrode is set as cathode, the maximum mass concentration at the nozzle throat is around 0.2, 0.1 and 0.05 respectively for arc current of 500A, 1000A and 1500A.
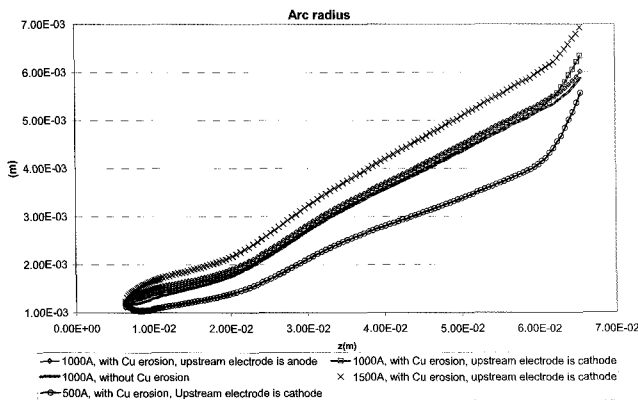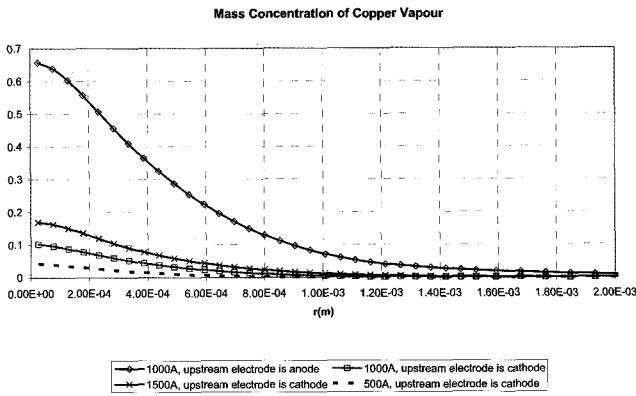

Fig. 5 The arc radius along the axial direction for I=500A, 1000A and 1500A when the upstream electrode is set as cathode. The effects of setting the upstream electrode as anode and the case without copper contamination are shown for the case of I=1000A
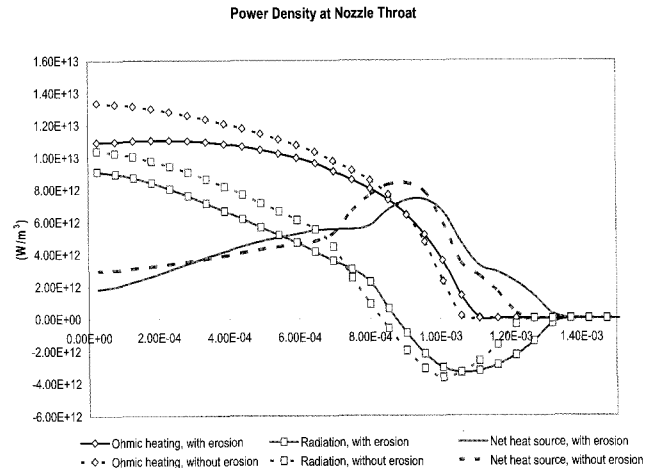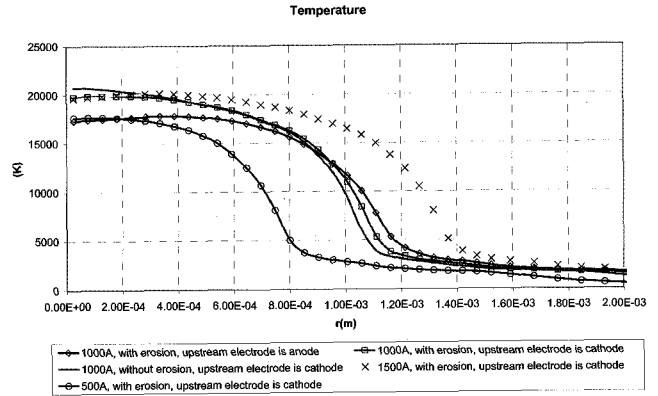

Fig. 6 The power density at the nozzle throat for I=1000A. The net heat source equals to ohmic heating minus radiation

For the arc current of 1000A, the arc radius is the smallest for the case without copper contamination under the same arc current. The presence of the copper vapour increases the radiation reabsorption region of the arc, and increases the temperature of the arc edge (as shown in Fig. 6). As a result, the arc radius increases. However, this increase of arc radius is not significant compared to the effects of arc current. When the upstream electrode is set to anode, the arc radius is larger and the mass concentration of the copper vapour is higher compared to the case where it is set to cathode for most of the arc except in the small region(around 4mm) in front of the downstream cathode electrode (Fig.5 and Fig.8). The maximum mass concentration of copper vapour is 0.65 and 0.1 at nozzle throat respectively for the case of anode and cathode upstream electrodes. Hence, for the same electrode, the evaporation rate is higher when it is set as anode compared to the case it is set to cathode. This phenomenon is consistent with experimental observations published in [18].
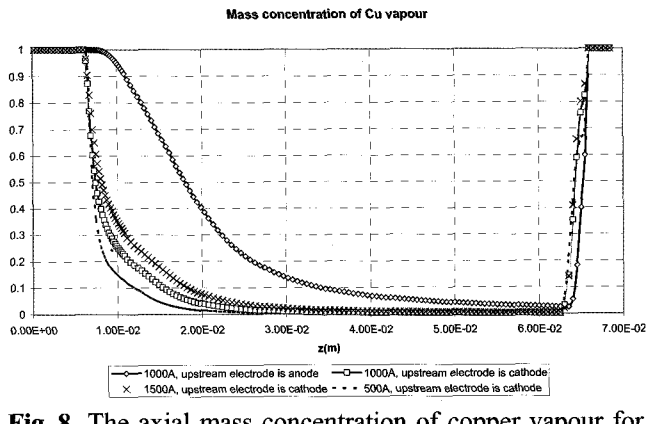
The effects of arc current, copper contamination and electrode polarity on the arc temperature are shown in Fig.s 9 and 10. Electrode vapour considerably affects the arc temperature. The arc temperature decreases rapidly in the region with high mass concentration of copper vapour as shown in Fig.s 8 and 9. This can be attributed to the increased of net emission coefficient of SF_6-Cu mixture which is considerably higher than that of pure SF_6 at the same temperature and pressure. The arc current also affects the temperature profiles, especially in the radial direction as shown in Fig. 10. With higher current, the ohmic heating increases, and this increases the arc temperature and arc radius. The maximum temperature that can be attained in the arc is around 21000K.
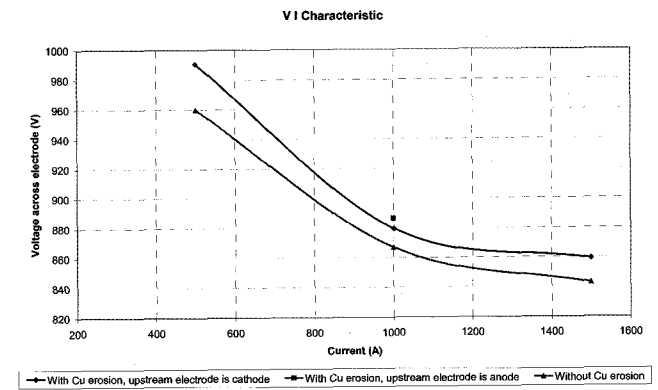
Fig. 7 The radial mass concentration of copper vapour for I=500A, 1000A and 1500A when upstream electrode set as cathode. The effect of setting the upstream electrode as anode is shown for the case of 1000A

Fig. 8 The axial mass concentration of copper vapour for I=500A, 1000A and 1500A when upstream electrode is set as cathode. The effect of setting the upstream electrode as anode is shown for the case of 1000A

Fig. 9 The axial distribution of arc temperature for I=500A, 1000A and 1500A when upstream electrode is set as cathode with copper contamination. The effect of setting the upstream electrode as anode and the case without copper contamination are shown for the case of 1000A
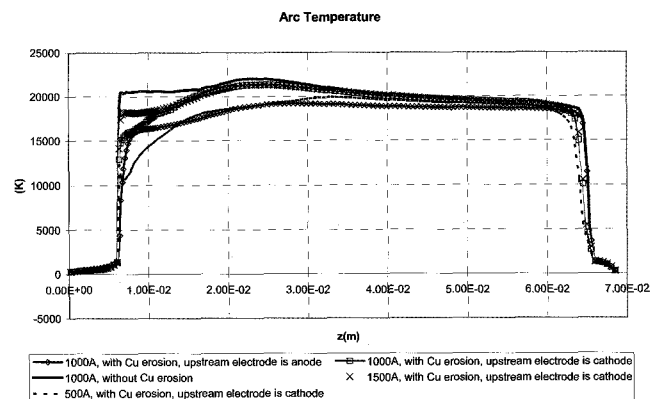

Fig. 10 The radial distribution of arc temperature for I=500A, 1000A and 1500A at nozzle throat when upstream electrode is set as cathode with copper contamination. The effect of setting the upstream electrode as anode and the case without copper contamination are shown for the case of 1000A


Fig. 11 The V-I characteristics of the arc with and without the consideration of copper contamination. The upstream electrode is set as cathode. The effect of setting upstream electrode as anode is also shown for the arc current of 1000A

The voltage-current characteristic of the arc is shown in Fig. 11. The voltage across the electrodes is not sensitive to the copper vapour as the difference is less than 4% for the arc current under consideration. The arc temperature and velocity at current zero are shown in Figs 12 and 13 respectively. The arc temperature is reduced considerably with maximum temperature of around 10000K. The maximum velocity is 2314m/s.

There is negligible mass concentration of copper vapours as the heat fluxes into the electrodes are insufficient to cause evaporation. As shown in Fig. 14, the lowest arc temperature at current zero is 8000K without the consideration of copper contamination, compared to 8400K for the case with copper contamination. The arc radius at current zero at the position with lowest arc temperature with copper contamination are10% and 4% bigger for the case of anode and cathode upstream electrodes respectively
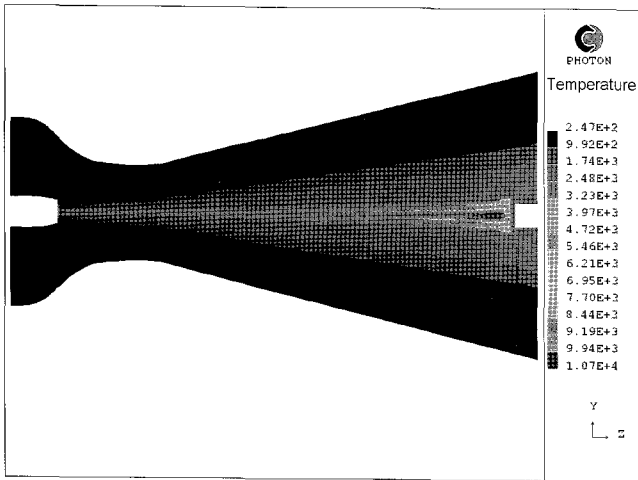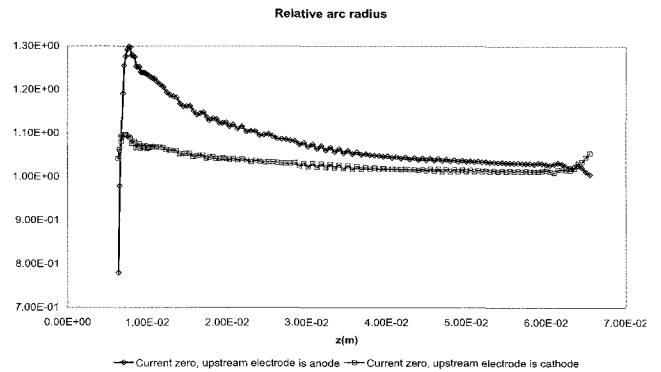
Fig. 12 The temperature distribution of the arc at current zero. dI/dt=27μA/s The upstream electrode is set as cathode
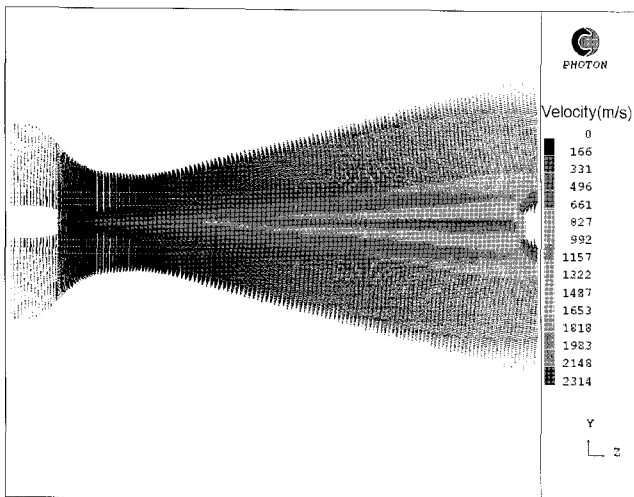
Fig. 13 The velocity vector of the arc at current zero. dI/dt=27μA/s The upstream electrode is set as cathode
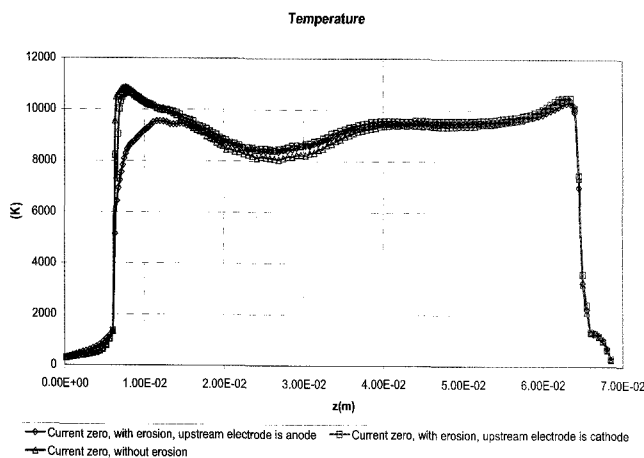
Fig. 14 The effects of electrode polarity and copper contamination on the arc temperature at current zero, . dI/dt=27μA/s

Fig. 15 The relative arc radius with copper contamination at current zero for different electrode polarity with respect to the arc radius at current zero without copper contamination

compared to the case without copper contamination as shown in Fig. 15. As a result, it is predicted that the interruption capability of the circuit breaker is reduced with the effects of erosion as the arc temperature is higher and arc radius is bigger in the presence of copper vapours at current zero.

4. Conclusion

The influence of copper vapour due to electrode erosion on the arc in a simple Laval nozzle inside a circuit breaker has been simulated. Firstly, steady state simulations of the arc show the presence of copper vapours reduces the arc temperature but increases the arc radius due to the strong cooling mechanisms from the radiation losses. The arc radius is the most affected by the arc current. The polarity of the electrode affects the electrode evaporation process. The copper vapour concentration around the upstream electrode is higher compared to the downstream electrode because the copper vapour cannot diffuse against the high speed flow of the arc in the downstream electrode. The total arc voltage is not seriously affected by the copper vapour, typically less than 4% for the range of arc current from 500 to 1500A. Transient simulations have been performed in order to predict the arc behaviour at current zero. With the consideration of copper contamination, a higher arc temperature and bigger arc radius is predicted at current zero compared to the case of without copper contamination. It is therefore predicted that the interruption capability of the circuit breaker is reduced resulting from the electrode erosion processes.

References

[1]   D. R. Airey, "A rapid-scanning polychromator for

time-resolved temperature and radius measurements in 40 kA SF6 arc," *J. Phys. D*, Vol. 12, pp.379-402, 1979.

[2] M. Bouaziz, M. Razafinimanana, J. J. Gonzalez and A. Gleizes, "An Experimental and Theoretical Study of the Influence of Copper Vapour on a SF6 Arc Plasma at Atmospheric Pressure," *J. Phys. D*, Vol. 31, pp.1570-1577, 1998.

[3] K. D. Song, B. Y. Lee, K. Y. Park and J. H. Park, "Analysis of Thermal Recovery Characteristics for SF6 Gas-Blast Arc within Laval Nozzle," Trans. on KIEE, Vol. 51, No. 9, pp.522-529, 2002.

[4] B. Y. Lee, K. D. Song, J. K. Chong and K. Y. Park, "Steady State Analysis of Nozzle Ablation under High Temperature and High Pressure Arc Plasma," Trans. on KIEE, Vol.52, No. 9, pp.395-399, 2003.

[5] B. Y. Lee, K. D. Song, J. K. Chong and K. Y. Park, "Analysis of Thermal Recovery Characteristics for Nozzle of SF6 GCB Considering Nozzle Ablation," Trans. on KIEE, Vol.54, No.2, pp.76-82, 2005.

[6] Sang-Hun Pakr, Chae-Yoon Bae, Hyun-Kyo Jung, "Hot Gas Analysis of Circuit Breakers By Combining Partial Characteristic Method with Net Emission Coefficient," KIEE   International Trans. on EMECS, Vol. 3 No. 3, pp. 115 – 121, 2003.

[7] J. L. Zhang, J. D. Yan and M. T. C. Fang, "Electrode evaporation and its effects on thermal arc behavior," *IEEE Trans. on Plasma Sci.*, Vol. 32, pp.1352-1361, 2004.

[8] S. S. Ciobanu, P. Chevrier and C. Fleurier, *XXIII Int. Conf. On Phenomena in ionized gases*, Vol. 2, pp. 100-101, 1997.

[9] H. Ikeda, G. R. Jones, M. Irie and A. N. Prasad, *VIIth Int. Conf. on Gas Disch. And their Applic*, pp.5, 1982.

[10] G. Frind, R. E. Kinsinger, R. D. Miller, H. T. Nagamatsu and H. O. Noeske, "Fundamental investigation of arc interruption in gas flows," *EPRI EL 284 final report*, Sec.5 pp.2-3, 1977.

[11] Coufal O , "Thermophysical properties of the reacting mixture SF6 and Cu in the range 3000 to 50,000K and 0.1 to 2.0MPa, Part2: Thermodynamic properties," *Acta Techn. CSAV*, 37, pp.371–397, 1992.

[12] B. Chervy, A. Gleizes and M. Razafinimanana, "Thermodynamic properties and transport coefficients in SF6-Cu mixtures at temperatures of 300-30000K and pressures of 0.1-1MPa," *J. Phys. D*, 27, pp.1193-1206, 1994.

[13] P. Krenek, "Thermophysical properties of the reacting mixture SF6 and Cu in the range 3000 to 50000K and 0.1 to 2MPa Part 3: Transport Properties," *Acta Techn. CSAV*, 37, pp.399-410, 1992.

[14] J. F. Zhang, M. T. C. Fang and D. B. Newland,

"Theoretical investigation of a 2kA arc in a supersonic nozzle," *J. Phys. D*, 20, pp.368-379, 1987.

[15] A. Gleizes, J. J. Gonzalez, B. Liani and G. Raynal, "Calculation of net emission coefficient of thermal plasmas in mixtures of gas with metallic vapour," *J. Phys. D*, 26, pp.1921-1927, 1993.

[16] J. D. Yan, K. I. Nuttall and M. T. C. Fang, "A comparative study of turbulence models for SF6 arcs in a supersonic nozzle," *J. Phys. D*, 32, pp.1401-1406, 1999.

[17] K. D. Song, B. Y. Lee and K. Y. Park, "Analysis of thermal recovery for SF6 gas-blast arc within laval nozzle," *Jpn. J. Appl. Phys.*, 42, pp.7073-7079, 2003.

[18] J. Tepper, M. Seeger, T. Votteler, V. Behrens and T. Honig, "Prediction of the erosion of arcing contacts in high-voltage circuit breakers," *XV International conference on gas discharges and their applications*, Toulouse, Vol.1, pp.105-108, 2004.

Vui-Kien Liau
He received B.Eng and Ph.D degrees in electrical engineering from Liverpool University, UK in 2000 and 2004 respectively. His research interests are arc modeling, non-equilibrium plasma, microwave plasma, and circuit breakers.
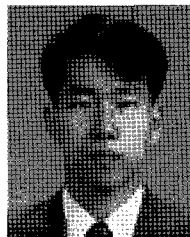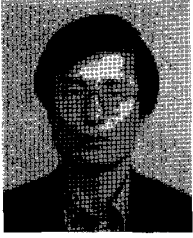

Byeong-Yoon Lee
He received the B.S, M.S and Ph.D degree in electrical engineering from Seoul National University in 1990, 1992 and 1997 respectively. Since 1996, he has been with KERI, as a senior research engineer in the advanced power apparatus research group. His research interests are flow field analysis, electric & magnetic analysis and arc phenomena in gas circuit breakers.

Ki-Dong Song
He received the B.S and M.S degree in electrical engineering from Inha University in 1988 and 1990 respectively. Since 1990, he has been with KERI, as a senior research engineer in the advanced power apparatus research group. His research interests are flow field analysis, design parameters and measuring techniques in gas circuit breakers.

Kyong-Yop Park

He received the B.S degree in electrical engineering from Seoul National University in 1979, the M.S and Ph.D degree from Liverpool Univrsity, U.K. Since 1981, he has been with KERI, as a executive director of the advanced power apparatus research group. His research interests are flow field analysis, analysis of test results and arc phenomena in gas circuit breakers.